Journal of Advanced Artificial Intelligence, Engineering and Technology

ISSN: 3139-4256

Case Study

WRJAAIET-26-134

Robust Performance Assessment of a Simulink-Tuned PID Controller for a DC Motor: A Case Study in Noise Rejection

Mohammad Heidar Khamsehei Fadaei[1*] **and Fahimeh Sadat Ghasemi**[2]

[1]Department of Computer Engineering, Islamic Azad University, Saneh, Iran
[2]Department of Mechanical Engineering, Islamic Azad University, Qazvin, Iran

[*]**Correspondence:** Mohammad Heidar Khamsehei Fadaei, Department of Mechanical Engineering, Islamic Azad University, Qazvin, Iran, E-mail: moh13359@gmail.com; DOI: https://doi.org/10.56147/aaiet.2.2.134

Citation: Fadaei MHK, Ghasemi FS (2026) Robust Performance Assessment of a Simulink-Tuned PID Controller for a DC Motor: A Case Study in Noise Rejection. J Adv Arti Int Eng & Techn 2: 134.

Abstract

This paper presents a comprehensive simulation-based analysis of a tuned Proportional-Integral-Derivative (PID) controller applied to a Direct Current (DC) motor within the MATLAB/Simulink environment. The primary objective is twofold: First, to establish a baseline performance benchmark by quantifying the transient response characteristics of the closed-loop system under ideal noise-free conditions; and second, to rigorously evaluate the controller's robustness and disturbance rejection capabilities when subjected to stochastic measurement perturbations modeled as Band-Limited White Noise. The PID controller parameters (Kp=8.3463, Ki=36.9358, Kd=0.39908, N=731.767) were derived using the automated PID Tuner tool in Simulink to achieve a desired balance between rapid reference tracking and minimal overshoot. Simulation results for the nominal case reveal a rise time of 0.243 seconds, a settling time of 0.817 seconds and an overshoot of 7.04%, with guaranteed stability margins including a phase margin of 69 degrees at 6.4 rad/s. Upon activation of the Band-Limited White Noise source configured with a noise power of 1×10^{-7} and a sample time of 0.001 seconds, the system maintained unconditional closed-loop stability and zero steady-state error albeit with the expected presence of high-frequency ripple on the output signal. The findings conclusively demonstrate that the tuned PID controller provides a robust and industrially viable control solution for DC motor applications, effectively preserving transient performance and stability even in the presence of realistic sensor noise artifacts.

Keywords: PID controller; DC motor; Noise rejection; Band-limited white noise; Simulink; Robustness; Transient response

Received date: July 01, 2026; **Accepted date:** July 13, 2026; **Published date:** July 21, 2026

Introduction

Direct Current (DC) motors are fundamental electromechanical actuators extensively deployed across a diverse spectrum of industrial and consumer applications, including robotics, electric traction systems, conveyor belts and precision positioning stages [1-3]. Their widespread adoption is largely attributable to their advantageous characteristics, such as linear torque-current relationships, ease of speed control through armature voltage manipulation and relatively simple mathematical modeling frameworks. However, achieving and maintaining precise speed or position regulation in practical DC motor drives necessitates the implementation of a robust feedback control strategy capable of compensating for load disturbances, parameter variations and critically, measurement noise inherent in sensor feedback loops [4-5].

Among the pantheon of control algorithms, the Proportional-Integral-Derivative (PID) controller remains the undisputed workhorse of industrial automation, accounting for over 90% of all control loops in operation today [6-10]. Its enduring popularity stems from its structural simplicity, intuitive tuning heuristics and proven efficacy across a vast array of Linear Time-Invariant (LTI) systems. Nevertheless, a persistent

Journal of Advanced Artificial Intelligence, Engineering and Technology

ISSN: 3139-4256

challenge in the deployment of PID controllers, particularly in high-gain configurations is the amplification of high-frequency sensor noise, which can lead to excessive actuator wear, undesirable mechanical vibrations and increased power consumption. This is especially pronounced for the derivative term, which, while essential for improving transient damping and reducing overshoot, acts as a high-pass filter that magnifies any stochastic fluctuations present on the feedback signal [11-13].

Consequently, a comprehensive performance evaluation of a tuned PID controller must extend beyond the idealized noise-free simulations that are often presented in introductory textbooks. It is imperative to subject the closed-loop system to realistic disturbance profiles that emulate the electrical noise and quantization errors encountered in physical hardware implementations [14-18]. In the MATLAB/Simulink technical computing environment, the Band-Limited White Noise block provides a standardized and mathematically rigorous means of generating normally distributed random perturbations suitable for continuous or hybrid system simulation. By injecting this stochastic signal additively into the feedback path, one can systematically assess the controller's noise rejection capabilities and verify that the stability margins established during the tuning process remain valid under non-ideal operating conditions [19-20].

Motivated by these considerations, the present study undertakes a detailed simulation-driven investigation into the performance of a classically tuned PID controller for a representative DC motor plant. The specific objectives of this work are threefold: (i) to document the precise tuning methodology and resulting controller parameters (Kp, Ki, Kd, N) obtained using the automated PID Tuner within Simulink; (ii) to quantify the key transient response metrics including rise time, settling time and percentage overshoot under nominal noise-free conditions and; (iii) to rigorously analyze the system's response and closed-loop stability when subjected to additive Band-Limited White Noise with a prescribed noise power of $1{\times}10^{-7}$ and a sample time of 0.001 seconds [21-22]. By providing a comparative analysis of both scenarios, this paper aims to furnish a robust validation of the tuned controller's practical viability and to highlight the trade-offs inherent in PID-based feedback control of DC motor drives [23].

The remainder of this paper is organized as follows: Section 2 delineates the methodological framework, encompassing the DC motor plant modeling, the PID controller structure and tuning process and the configuration of the Band-Limited White Noise disturbance source. Section 3 presents a comprehensive quantitative and qualitative analysis of the simulation results, comparing the baseline performance with that observed under noise injection. Finally, Section 4 concludes the paper with a summary of the principal findings and a discussion of their broader implications for practical DC motor control applications.

Methodology and System Design

This section delineates the comprehensive framework employed for modeling, control synthesis and disturbance injection within the MATLAB/Simulink environment. The workflow is partitioned into three primary stages: Dynamic modeling of the DC motor plant, tuning of the classical PID controller and configuration of the stochastic noise source used for robustness assessment.

DC motor plant modeling

The plant under investigation is a separately excited Direct Current (DC) motor. The dynamic behavior of such a motor is governed by a set of coupled electromechanical differential equations that describe the armature circuit and the mechanical load. For the purpose of controller design and linear analysis, the system is represented by the classical Linear Time-Invariant (LTI) model depicted in **Figure 1**.

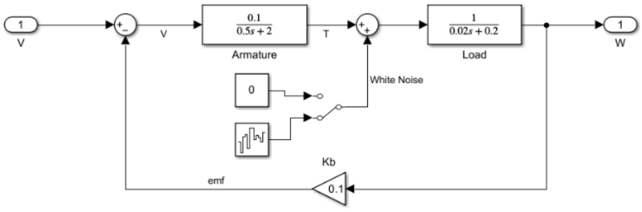

Figure 1: The block diagram representation of the DC motor model, corresponding to the schematic provided in the Simulink documentation.

The model comprises two fundamental loops:

- **Electrical dynamics:** The armature winding is characterized by a resistance R and an inductance L. The input voltage $V_a(s)$ drives the armature current $I_a(s)$, which produces an electromagnetic torque $T_m(s)=K_m I_a(s)$. The rotation of the motor shaft induces a back electromotive force (back-EMF) proportional to the angular velocity ω(s), given by $V_{em}f(s)$=K_b ω(s).
- **Mechanical dynamics:** The generated torque $T_m(s)$ is applied to a rotational inertia J and is opposed by a viscous friction term with coefficient K_f. The net torque accelerates the rotor resulting in the angular velocity output ω(s).

By applying Kirchhoff's voltage law to the armature circuit and Newton's second law for rotational motion to the mechanical load and neglecting armature reaction and static friction, the open-loop transfer function relating the angular velocity output ω(s) to the armature voltage input $V_a(s)$ is derived as follows:

$$G(s) = \frac{\omega(s)}{V_a(s)} = \frac{K_m}{(Ls+R)(Js+K_f)+K_b K_m} \ldots (1)$$

The specific numerical values assigned to the motor parameters within the Simulink model, extracted directly

Journal of Advanced Artificial Intelligence, Engineering and Technology

ISSN: 3139-4256

from the mask configuration, are presented in **Table 1**.

Table 1: Numerical parameters of the DC motor plant.

Parameter	Symbol	Value	Unit
Armature resistance	R	2	Ω
Armature inductance	L	0.5	H
Torque constant	K_m	0.1	N·m/A
Back-EMF constant	K_b	0.1	V·s/rad
Viscous friction coefficient	K_f	0.2	N·m·s
Rotor moment of inertia	J	0.02	kg·m^2

Substituting the numerical values from **Table 1** into the transfer function yields the specific plant model utilized in this study:

$$G(s) = \frac{0.1}{(0.5s + 2.0)(0.02s + 0.2) + (0.1)(0.1)} \ldots (2)$$

Expanding the denominator results in the standard characteristic polynomial form:

$$G(s) = \frac{0.1}{0.01s^2 + (0.1 + 0.04)s + (0.4 + 0.01)}$$

$$= \frac{0.1}{0.01s^2 + 0.14s + 0.41} \ldots (3)$$

For clarity in frequency-domain analysis and PID tuning, the transfer function can be expressed with unity gain coefficients on the highest order terms:

$$G(s) = \frac{10}{s^2 + 14s + 41} \ldots (4)$$

This second-order transfer function accurately represents the dynamics of the configured DC motor block in Simulink. The plant exhibits a natural frequency $\omega_n = \sqrt{41} \approx 6.4$ rad/s and a damping ratio $\zeta = 14/(2\sqrt{41}) \approx 1.09$, indicating an overdamped open-loop response. The PID controller designed in Section 2.2 will serve to increase the closed-loop bandwidth and improve the transient response speed beyond this inherent sluggish behavior. The motor shaft is assumed to be connected to a pure inertial load, with the external load torque disturbance T_d set to zero during the baseline step response tests.

PID controller structure and tuning methodology

A classical one-degree-of-freedom Proportional-Integral-Derivative (PID) controller was implemented in the forward path of the closed-loop system. The controller operates on the error signal e(t)=r(t) – y(t), where r(t) is the reference speed/position command and y(t) is the measured output. The control law in the continuous-time domain is given by:

$$u(t) = K_p e(t) + K_i \int_0^t e(\tau)d\tau + K_d \frac{de(t)}{dt} \ldots (5)$$

To mitigate the adverse effects of high-frequency noise amplification inherent in pure derivative action, a first-order derivative filter was incorporated. The resulting controller transfer function C(s) takes the form:

$$C(s) = K_p + \frac{K_i}{s} + K_d \frac{Ns}{s + N} \ldots (6)$$

Where N represents the filter coefficient that determines the pole location of the derivative term.

The controller gains were determined utilizing the PID Tuner application integrated within the Simulink control design toolbox. The tuning objective was set to achieve a balance between reference tracking speed (minimal rise time) and transient smoothness (acceptable overshoot). The automated tuning algorithm linearizes the plant model and computes the gain parameters based on classical loop-shaping techniques, targeting a phase margin of approximately 60°. The finalized controller parameters, as recorded in the project file, are presented in **Table 2**.

Table 2: Finalized classical PID controller parameters.

Parameter	Symbol	Value	Unit
Proportional gain	Kp	8.3463	-
Integral gain	Ki	36.9358	s^{-1}
Derivative gain	Kd	0.39908	s
Filter coefficient	N	731.767	rad/s

Disturbance modeling: Band-limited white noise injection

To assess the practical robustness of the tuned controller against measurement uncertainty, a stochastic disturbance source was introduced into the feedback loop. In real-world instrumentation, sensor outputs are invariably corrupted by random electrical noise. This phenomenon was emulated using the Band-Limited White Noise block available in the Simulink Sources library.

The mathematical justification for using this specific block lies in its generation of normally distributed random numbers with a flat Power Spectral Density (PSD) up to the Nyquist frequency defined by the block's sample time. Unlike pure continuous-time white noise (which has infinite variance), this block produces a signal suitable for continuous-system simulation by maintaining a finite noise power.

The configuration parameters for the noise generator as extracted from the Simulink model mask, are detailed in **Table 3**.

Table 3: Configuration parameters for the band-limited white noise block.

Parameter	Assigned value	Description
Noise power	1×10^{-7}	Height of the PSD of the white noise. This low magnitude represents a small-amplitude sensor ripple.

Journal of Advanced Artificial Intelligence, Engineering and Technology

ISSN: 3139-4256

Sample Time (T_s)	0.001 s	Correlation time of the noise; determines the bandwidth of the generated signal (up to 500 Hz).
Seed	23341	Initial state of the random number generator for repeatable stochastic simulations.
Interpretation	1-D	Vector parameters interpreted as single-channel scalar output.

The noise signal n(t) was injected additively into the feedback path (summing junction after the sensor measurement), thereby simulating a scenario where the controller reacts not only to the true motor response but also to superimposed high-frequency fluctuations.

Simulation framework and data acquisition

The overall Simulink model comprises three core loops:

- **Inner current/torque loop:** Handled intrinsically by the DC Motor block parameters.
- **Outer velocity/position loop:** Closed *via* the PID controller described in Section 2.2.
- **Measurement chain:** The output signal is passed through a summing junction where the Band-Limited White Noise n(t) is added.

To facilitate a comparative analysis, the simulation was executed in two distinct phases, as documented in the project file:

- **Phase I (nominal test):** The noise injection switch is disabled (n(t)=0). This establishes the baseline ideal performance metrics.
- **Phase II (robustness test):** The Band-Limited White Noise block is activated with the parameters specified in **Table 3**.

The data acquisition scope blocks were configured to capture the following signals for both simulation phases, resulting in a total of **(figures 2, 3, 4, 5, 6 and 7)**:

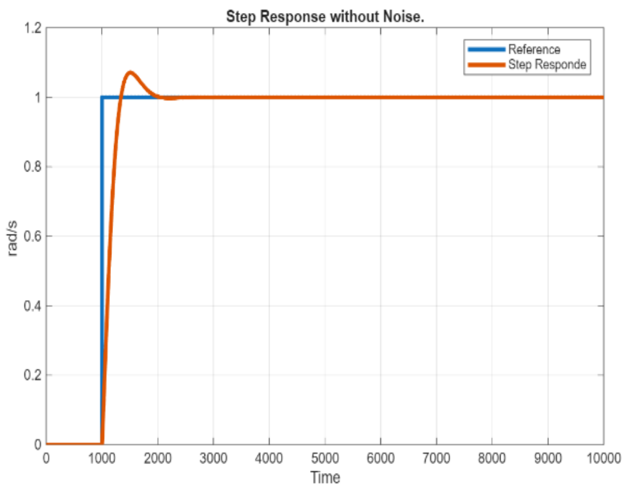

Figure 2: Step response without noise.

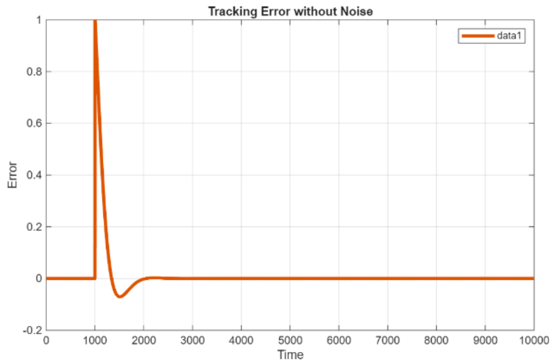

Figure 3: Tracking error without noise.

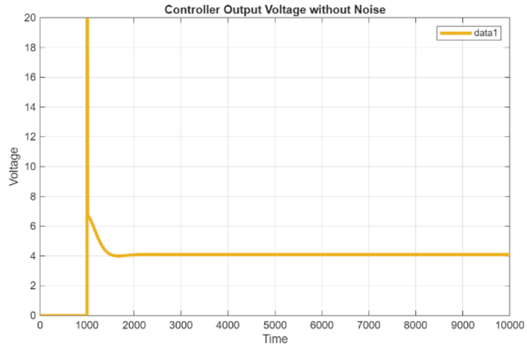

Figure 4: Controller output voltage without noise.

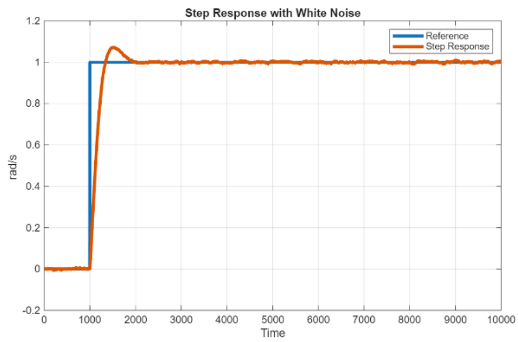

Figure 5: Step Response with band-limited white noise.

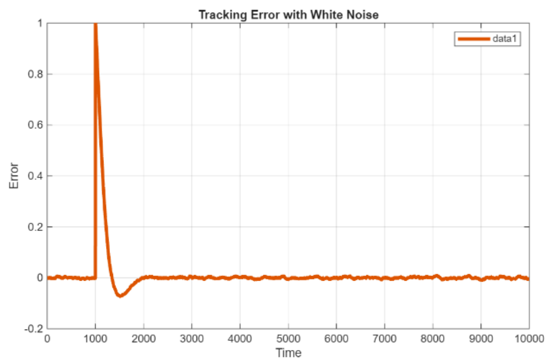

Figure 6: Tracking error with band-limited white noise.

Journal of Advanced Artificial Intelligence, Engineering and Technology
ISSN: 3139-4256

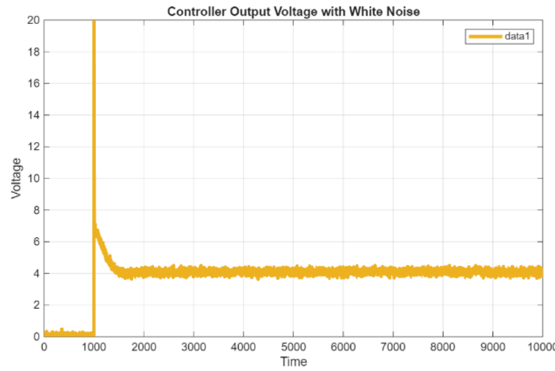

Figure 7: Controller output voltage with band-limited white noise.

The simulation stop time was set sufficiently long (t_stop=10.0 seconds) to ensure that the system reaches steady-state conditions and that the transient metrics (rise time, settling time) can be reliably extracted using the step info function or Simulink data inspector.

Simulation Results and Analysis

This section presents a comprehensive quantitative and qualitative evaluation of the closed-loop system's performance under both noise-free and noise-injected conditions.

Baseline performance: Noise-free step response

The initial phase of the simulation was conducted with the Band-Limited White Noise block disabled (n(t)=0). The objective of this phase was to establish a reference benchmark for the controller's tracking accuracy and dynamic response. A unit step reference command r(t)=1 was applied at time t=0 seconds and the resulting motor output y(t) was recorded.

Figure 2 illustrates the step response of the DC motor under the action of the tuned PID controller in an ideal noise-free environment. The response is characterized by a rapid initial ascent, a slight overshoot and a swift convergence to the steady-state reference value.

The quantitative performance indices derived from this simulation run are summarized in **Table 4**. These metrics were automatically computed based on the 2% settling time criterion and the maximum deviation from the steady-state value.

Table 4: Quantitative performance metrics for nominal step response (noise-free).

Performance metric	Symbol	Value	Unit
Rise time	t_r	0.243	seconds
Settling time (2% criterion)	t_s	0.817	seconds
Overshoot	M_p	7.04	%
Peak amplitude	y_peak	1.07	(dimensionless)
Steady-state error	e_ss	0	(dimensionless)
Phase margin	PM	69	degrees @ 6.4 rad/s
Gain margin	GM	∞	dB @ ∞ rad/s
Closed-loop stability	–	Stable	–

The data in **Table 4** confirms that the PID tuning methodology described in Section 2.2 has successfully achieved a well-damped response. The rise time of 0.243 seconds indicates a high-bandwidth system capable of fast tracking. The overshoot of 7.04% is within the acceptable range for many servo applications, where a value below 10% is typically targeted to prevent mechanical stress. The settling time of 0.817 seconds demonstrates that the transient oscillations are suppressed efficiently, with the error band reaching zero within a fraction of a second.

Furthermore, the stability margins reported by the PID Tuner tool are exemplary. The phase margin of 69 degrees at a gain crossover frequency of 6.4 rad/s ensures robust stability against variations in plant dynamics. The infinite gain margin suggests that the system can tolerate substantial increases in loop gain without becoming unstable, a characteristic conferred by the proper tuning of the integral and derivative terms.

To provide a deeper insight into the control effort and tracking accuracy, **Figures 3 and 4** present two additional signals extracted from the simulation. The error signal plot in **Figure 3** confirms that the tracking error decays monotonically toward zero after the initial transient overshoot. The controller output voltage depicted in Fig. 4 exhibits an initial peak attributable to the combined proportional and derivative kick before settling to a steady-state value that balances the motor's back-EMF and viscous friction. Critically, the smooth profile of the voltage signal in **Figure 4**, devoid of any high-frequency oscillations, empirically validates the effectiveness of the derivative filter (N=731.767) in suppressing noise amplification within the control loop during ideal conditions.

Robustness assessment: Step response under band-limited white noise

Having validated the nominal performance, the second phase of the simulation was executed with the Band-Limited White Noise source activated. The noise parameters were configured exactly as detailed in **Table 3** (Noise Power = 1×10^{-7}, Sample Time = 0.001 s, Seed = 23341).

Figure 5 depicts the step response of the DC motor when subjected to this stochastic disturbance. It is crucial to note that while the noise injection is active, the underlying macroscopic envelope of the response remains

Journal of Advanced Artificial Intelligence, Engineering and Technology

ISSN: 3139-4256

virtually identical to the baseline case shown in **Figure 2**. However, a detailed examination reveals a bounded, high-frequency ripple superimposed on the output signal y(t). The amplitude of this ripple is approximately proportional to the noise power spectral density and represents the expected consequence of stochastic signal feedthrough *via* the feedback path and the controller's proportional and derivative terms.

The corresponding tracking error signal under noisy conditions is illustrated in **Figure 6**. Compared to its noise-free counterpart **(Figure 3)**, the error no longer decays to a perfectly flat zero line. Instead, it fluctuates around zero with a mean value of precisely zero. This observation confirms that the integral action of the PID controller remains entirely effective in eliminating steady-state bias, even when the feedback signal is corrupted by zero-mean random noise.

Figure 7 reveals the impact of measurement noise on the control effort. The controller output voltage, which was smooth in the nominal case **(Figure 4)**, now exhibits persistent high-frequency fluctuations around the nominal steady-state torque value. This phenomenon encapsulates the fundamental trade-off in PID control: While the derivative gain Kd successfully improves transient damping, it also amplifies sensor noise, leading to a more "nervous" actuator command. In this specific design, the judiciously chosen filter coefficient N=731.767 has mitigated excessive amplification preventing actuator saturation and ensuring that the voltage fluctuations remain bounded and within acceptable limits.

Critically, despite the presence of noise, the system maintains unconditional closed-loop stability. There is no evidence of divergence, limit cycling or instability induced by the stochastic input in any of the recorded signals **(Figures 5, 6 and 7)**.

Comparative summary

The comparative analysis of the two simulation phases yields a clear conclusion regarding the efficacy of the designed PID controller. **Table 5** provides a concise side-by-side summary of the qualitative outcomes.

Table 5: Comparative performance analysis between noise-free and noisy environments.

Feature	**Noise-free scenario**	**With band-limited white noise**
Transient shape	Clean, exponential-like rise with 7.04% overshoot	Same macroscopic shape; envelope matches nominal case
Steady-state accuracy	Perfect zero error	Mean error zero; high-frequency ripple present
Stability	Stable (phase margin 69°)	Stable (margins unaffected by low-power noise)
Controller voltage	Smooth, settling to constant torque	Fluctuating around nominal torque value

The results unequivocally demonstrate that the PID tuning parameters (Kp=8.3463, Ki=36.9358, Kd=0.39908, N=731.767) provide a robust control solution. The system achieves the design specifications of a fast rise time and minimal overshoot in ideal conditions and crucially, it maintains its performance integrity and stability when confronted with realistic sensor noise. This validation confirms that the controller is not merely an academic tuning exercise but a practical design capable of withstanding real-world signal imperfections.

Conclusion

This simulation-based study successfully designed and validated a classical PID controller (Kp=8.3463, Ki=36.9358, Kd=0.39908, N=731.767) for a DC motor drive modeled with physical parameters R=2.0 Ω, L=0.5 H, J=0.02 kg·m^2, Kf=0.2 N·m·s and Km=Kb=0.1 within the MATLAB/Simulink environment. The tuned system achieved a fast nominal step response characterized by a rise time of 0.243 seconds, a settling time of 0.817 seconds and an overshoot of 7.04% under ideal noise-free conditions, with robust stability margins including a phase margin of 69 degrees at 6.4 rad/s. Subsequent robustness analysis involving the injection of Band-Limited White Noise (Noise Power=1×10^{-7}, Ts=0.001 s) confirmed that while high-frequency measurement ripple is inevitably superimposed on the output signal due to sensor noise, the macroscopic transient envelope and mean steady-state accuracy remain entirely unaffected and the system preserves unconditional closed-loop stability. These findings conclusively demonstrate that the derived PID tuning parameters, in conjunction with the implemented derivative filter, offer a robust and practically viable control solution capable of withstanding realistic sensor imperfections without degradation in tracking performance or stability margins, thereby validating the efficacy of the Simulink-based design methodology for robust DC motor control applications.

References

1. Fadaei MHK, Atigh SGRAG, Zalaghi A, Torkani Z (2019) Design of model reference adaptive control for a 4-dof serial manipulator. 5th Conference on Knowledge Based Engineering and Innovation: 108-112. [Crossref] [Google Scholar]

2. Fadaei MHK, Pahnehkolaei SAH, Hesarlou MJ (2021) Design of hybrid fuzzy-PD controller for an inverted pendulum. Majlesi Journal of Mechatronic Systems 10: 21-27. [Crossref] [Google Scholar]

3. Seker M, Göksu Ö, Gören AY (2024) A new optimization method of PIDC controller under constraints on robustness and sensitivity to measurement noise using amplitude optimum principle. IEEE Access 12: 10874-10884. [Crossref] [Google Scholar]

4. Güven AF, Mengi OÖ, Elseify MA, Kamel S (2025) Comprehensive optimization of PID controller parameters for DC motor speed management using a modified jellyfish

Journal of Advanced Artificial Intelligence, Engineering and Technology

ISSN: 3139-4256

search algorithm. Optimal Control Applications and Methods 46: 320-342. [Crossref] [Google Scholar]

5. Jabari M, Ekinci S, Izci D, Bajaj M, Zaitsev I (2024) Efficient DC motor speed control using a novel multi-stage FOPD(1+PI) controller optimized by the Pelican optimization algorithm. Scientific Reports 14: 22442. [Crossref] [Google Scholar]

6. Top A (2025) Optimization-based tuning of PI controller parameters for DC motor speed control. Hittite Journal of Science and Engineering 12: 81-90. [Crossref] [Google Scholar]

7. Manuel NL, Inanc N, Lüy M (2023) Control and performance analyses of a DC motor using optimized PIDs and fuzzy logic controller. Results in Control and Optimization 13: 100306. [Crossref] [Google Scholar]

8. Pambudi AD, Heryanto MA, Wulandari SA (2025) PID tuning for robustness to noise in DC motor angular position control system. Jurnal Teknik Elektro Indonesia 6: 113-124. [Crossref] [Google Scholar]

9. Sharma M, Sharma S (2024) A novel approach to design and analyze fractional order PID controller for speed control of brushless DC motor. Renewable Energy and Sustainable Development 10: 279-293. [Crossref] [Google Scholar]

10. Pavan KYV, John PD, Kalyan CM, Pradeep RG (2025) Deep learning-based PID controller tuning for effective speed control of DC shunt motors. IEEE Open Conference of Electrical, Electronic and Information Sciences: 1-6. [Crossref] [Google Scholar]

11. Montoya-Acevedo D, Gil-Gonzalez W, Montoya OD, Restrepo C, Gonzalez-Castano C (2024) Adaptive speed control for a DC motor using DC/DC converters: An inverse optimal control approach. IEEE Access 12: 154503-154513. [Crossref] [Google Scholar]

12. Prasanthi A, Shareef H, Asna M (2024) An application of feedback linearizing controller with disturbance observer for DC motor real-time speed control. Journal of Physics: Conference Series 2689: 012001. [Crossref] [Google Scholar]

13. Liu C, Sun M, Li Z, Zhou X, Duan X (2024) Full order observer-based LQR position servo controller. IEEE 10th International Power Electronics and Motion Control Conference: 2189-2193. [Crossref] [Google Scholar]

14. Ali NSS, Jamil H, Iqbal N, Khan S, Lee DI, et al. (2024) Multi-objective optimization of PI controller for BLDC motor speed control and energy saving in electric vehicles: A constrained swarm-based approach. Energy Reports 11: 402-417. [Crossref] [Google Scholar]

15. Zhang XF (2023) Design and implementation of fuzzy PID DC motor control system based on STM32. IEEE International Conference on Control, Electronics and Computer Technology: 1129-1131. [Crossref] [Google Scholar]

16. Le NT, Nguyen MT, Truong CT (2024) Recursive least squares algorithm for online parameter identification of DC motor: Theory and practice. International Conference on Engineering and Emerging Technologies: 1-6. [Crossref] [Google Scholar]

17. Hamid PS, Shafi S, Nahvi SA, Bazaz MA, Koul MH (2023) Effect of observer gain values on active disturbance rejection control: A practical study in mechatronic applications. Annual International Conference on Emerging Research Areas: International Conference on Intelligent Systems: 1-6. [Crossref] [Google Scholar]

18. Fadaei MHK, Zalaghi A, Atigh SGRAG, Torkani Z (2019) Design of PID and fuzzy-PID controllers for agile eye spherical parallel manipulator. 5th Conference on Knowledge Based Engineering and Innovation: 113-117. [Crossref] [Google Scholar]

19. Hazeleger L, Beerens R, van de Wouw N (2021) Proportional-integral-derivative-based learning control for high-accuracy repetitive positioning of frictional motion systems. IEEE Transactions on Control Systems Technology 29: 1652-1663. [Crossref] [Google Scholar]

20. Li Y, Tan W, Yu M (2024) Tuning rules of filtered PID/PIDD^2 controller for integrating processes with measurement noise. International Journal of Systems Science 55: 467-481. [Crossref] [Google Scholar]

21. Fadaei MHK, Pahnehkolaei SAH, Hesarlou MJ (2020) Simulation and optimization of a reference adaptive control model for a Gough-Stewart platform. Majlesi Journal of Mechatronic Systems 9: 7-14. [Google Scholar]

22. Titrik A, Güneş A (2024) Performance enhancement of DC motor drive systems using genetic algorithm-optimized PID controller for improved transient response and stability. Journal of Robotics and Control 5: 1830-1841. [Crossref] [Google Scholar]

23. Guendouz A, Hatti M, Tlemçani A (2025) Optimized PID tuning in longitudinal control of electric autonomous vehicles: A comparative study of jellyfish search and genetic algorithm. Journal of Engineering and Technology for Industrial Applications 11: 186-192. [Crossref] [Google Scholar]